IOP Publishing Physica Scripta
Phys. Scr. 94 (2019) 115510 (7pp) https://doi.org/10.1088/1402-4896/ab2a7d

Controllable optical switching in a closed-loop three-level lambda system

Dong Hoang Minh[1] **and Huy Bang Nguyen**[2]

[1] Institute of Research and Development, Duy Tan University, Da Nang 550000, Vietnam
[2] Vinh University, 182 Le Duan Street, Vinh City, Vietnam

E-mail: bangnh@vinhuni.edu.vn

Received 18 April 2019, revised 13 May 2019
Accepted for publication 18 June 2019
Published 21 August 2019

Abstract

We propose a model for optical switching in a closed-loop three-level lambda atomic system excited by two optical fields, coupling and probe lights, and by a microwave-driven field. A set of coupled Maxwell–Bloch equations for the atom-field system is numerically solved with a combination of the Runge–Kutta and finite difference techniques. It is shown that the transmitted probe light can be switched to a nearly square pulse train by switching the relative phase of the interacting fields or by switching the intensity of the microwave field. Furthermore, the switching mode between the probe field and relative phase can be anti-synchronous or synchronous, depending on the relative phase being modulated to $\pi/2$ and $3\pi/2$ or π and 2π, respectively. Also, the efficiency and the switching rate can be controlled by the microwave field, the relative phase and the intensity of the coupling field. Such a controllable optical switching model can be applied in the design of optical switching and amplification devices working at low light intensities.

Keywords: optical switching, electromagnetically induced transparency, phase control

(Some figures may appear in colour only in the online journal)

1. Introduction

The all-optical switch is an important component in high-speed optical communication networks and it has potential applications in quantum information systems and quantum computing [1]. In recent years, the advent of electromagnetically induced transparency (EIT) [2, 3] has provided an excellent technique for all-optical switching at low light levels [4–11]. The EIT medium reduces absorption [12–14] with steep dispersion. Therefore, EIT can enhance significantly the interaction time between light and matter or enhance nonlinear optical processes in the vicinity of atomic resonant frequencies [15–17], which may achieve high efficiency even at the single-photon level [18, 19]. EIT can also modify the propagation dynamics of light pulses, such as the formation and propagation of optical solitons [20–28].

In the study of quantum interference control, the relative phase of the applied fields and excitation configurations plays a central role. Particularly in the atomic configuration of quantum loop schemes, the relative phase can modify dramatically the linear and nonlinear optical properties. This leads to some interesting phenomena, e.g., phase control of EIT [29, 30], amplification without inversion [31], phase-sensitive atom localization [32], giant Kerr nonlinearity associated with self-phase modulation and cross-phase modulation [6, 33–35], transient behavior [36, 37], and optical switching and other phase-dependent coherent properties [38–45]. The studies show that the closed-loop configuration is phase-sensitive to quantum coherent controls. Thus, it delivers more control modes in optical switching. It is worth mentioning here that these works focused only on the stationary-state response of the medium, although the dynamical response is fundamental for the optical switching [35, 42]. Growing from this interest, in this work we propose to use a closed-loop three-level lambda system excited by a pump and probe optical fields together with a microwave for the generation of optical switching. The dynamics of the atom-field system is represented by Liouville and wave equations in which the switching regimes are investigated with a variation

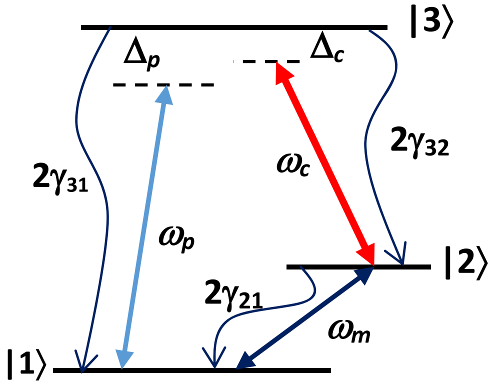

Figure 1. The excitation scheme of the closed-loop three-level lambda-type system.

of controlling parameters, such as relative phase and intensity of the coupling and microwave fields.

2. Model and basic equations

We consider a closed-loop three-level lambda-type atomic system as shown in figure 1. The transition $|3\rangle \leftrightarrow |2\rangle$ is driven by a coupling laser field with frequency ω_c, initial phase φ_c, and Rabi frequency $\Omega_c = \mu_{32}E_c/\hbar$. The transition $|3\rangle \leftrightarrow |1\rangle$ is excited by a probe field with frequency ω_p, initial phase φ_p, and Rabi frequency $\Omega_p = \mu_{31}E_p/\hbar$. A microwave field with a frequency ω_m and initial phase φ_m is used to couple levels $|2\rangle$ and $|1\rangle$ through a magnetic-dipole transition by a Rabi frequency $\Omega_m = \mu_{21}E_m/\hbar$. Here, $\mu_{ij} = \vec{\mu}_{ij}\vec{e}_L$ ($\vec{e}_L$ is the polarization unit vector of the laser field) denotes the dipole moment for the transition $|i\rangle$-$|j\rangle$. The microwave induces quantum coherence population of levels $|2\rangle$ and $|1\rangle$, which is important quantum interference. The spontaneous decay rate from level $|3\rangle$ to levels $|1\rangle$ and $|2\rangle$ is denoted by $2\gamma_{31}$ and $2\gamma_{32}$, respectively.

Using the rotating wave and the electric dipole approximations, the Hamiltonian of the system in the interaction picture can be written (with units of $\hbar = 1$) as [46]:

$$H_{\text{int}} = \begin{bmatrix} -\Delta_p & -\Omega_m^* e^{i\phi} & -\Omega_p^* \\ -\Omega_m e^{-i\phi} & -\Delta_c & -\Omega_c^* \\ -\Omega_p & -\Omega_c & 0 \end{bmatrix}, \tag{1}$$

where we denote frequency detunings $\Delta_p = \omega_{31}$–ω_p and $\Delta_c = \omega_{32}$-ω_c, and the relative phase ϕ of the applied fields is $\phi = (\omega_c + \omega_m - \omega_p)t + (\varphi_c + \varphi_m - \varphi_p)$.

Under the slowly varying envelope, and rotating wave and electric dipole approximations, the dynamics of the atom-field interaction is represented by the following Liouville and wave equations (in a local frame $\xi = z$ and $\tau = t$–z/c) [28, 46]:

$$\frac{\partial\rho_{11}}{\partial\tau} = 2\gamma_{31}\rho_{33} + i\Omega_p^*\rho_{31} - i\Omega_p\rho_{13} + i\Omega_m^* e^{i\phi}\rho_{21} - i\Omega_m e^{-i\phi}\rho_{12}, \tag{2a}$$

$$\frac{\partial\rho_{22}}{\partial\tau} = 2\gamma_{32}\rho_{33} - i\Omega_m^* e^{i\phi}\rho_{21} + i\Omega_m e^{-i\phi}\rho_{12} + i\Omega_c^*\rho_{32} - i\Omega_c\rho_{23}, \tag{2b}$$

$$\frac{\partial\rho_{33}}{\partial\tau} = -2(\gamma_{31} + \gamma_{32})\rho_{33} - i\Omega_p^*\rho_{31} + i\Omega_p\rho_{13} - i\Omega_c^*\rho_{32} + i\Omega_c\rho_{23}, \tag{2c}$$

$$\frac{\partial\rho_{21}}{\partial\tau} = (i(\Delta_c - \Delta_p) - \gamma_{21})\rho_{21} - i\Omega_m e^{-i\phi}(\rho_{22} - \rho_{11}) - i\Omega_p\rho_{23} + i\Omega_c^*\rho_{31}, \tag{2d}$$

$$\frac{\partial\rho_{31}}{\partial\tau} = -(i\Delta_p + \gamma_{31} + \gamma_{32})\rho_{31} - i\Omega_p(\rho_{33} - \rho_{11}) + i\Omega_c\rho_{21} - i\Omega_m e^{-i\phi}\rho_{32}, \tag{2e}$$

$$\frac{\partial\rho_{32}}{\partial\tau} = -(i\Delta_c + \gamma_{31} + \gamma_{32})\rho_{32} - i\Omega_c(\rho_{33} - \rho_{22}) + i\Omega_p\rho_{12} - i\Omega_m^* e^{i\phi}\rho_{31}, \tag{2f}$$

$$\frac{\partial\Omega_p(\xi, \tau)}{\partial(\alpha\xi)} = i\gamma_{31}\rho_{31}(\xi, \tau), \tag{2g}$$

where $\rho_{ij} = \rho_{ij}^*$ $(i \neq j)$ and $\rho_{11} + \rho_{22} + \rho_{33} = 1$, respectively; $\alpha = \frac{\omega_p N\,|\,\mu_{31}\,|^2}{4\varepsilon_0 c\hbar\gamma_{31}}$ is the propagation constant; N is the atomic density in the medium; and ε_0 and c are the permittivity and the light speed in the vacuum, respectively.

3. Results and discussions

First of all, we consider the influences of the relative phase ϕ on the transient absorption and dispersive properties of the probe field by numerically solving the time-dependent density matrix equations (2a)–(2f) by a standard fourth-order Runge–Kutta method with the initial conditions $\rho_{11}(0) = 1$, $\rho_{22}(0) = 0$, $\rho_{33}(0) = 0$, and $\rho_{ij}(0) = 0$ for $i \neq j$ $(i, j = 1, 2, 3)$. For simplicity, all involving parameters are scaled by γ_{31}, and each interacting field resonances with the corresponding atomic transition, $\omega_c + \omega_m - \omega_p = 0$, $\Delta_p = \Delta_c = 0$. Thus, the relative phase is relevant only to the initial phase of the fields, namely, $\phi = \varphi_c + \varphi_m - \varphi_p$. In figure 2 we plot the absorption $\mathrm{Im}(\rho_{31})$ and dispersion $\mathrm{Re}(\rho_{31})$ for the probe field versus the relative phase ϕ. It shows that $\mathrm{Im}(\rho_{31})$ and $\mathrm{Re}(\rho_{31})$ change sinuously with a period of 2π. Furthermore, the absorption vanishes when the relative phase $\phi = k\pi$ $(k = 0, 1, 2\ldots)$ whereas it varies to a maximum absorption or a maximum amplification when relative phase $\phi = (2k + 1)\pi/2$. The closed-loop three-level lambda system can therefore be switched to act as an absorber or amplifier by tuning the

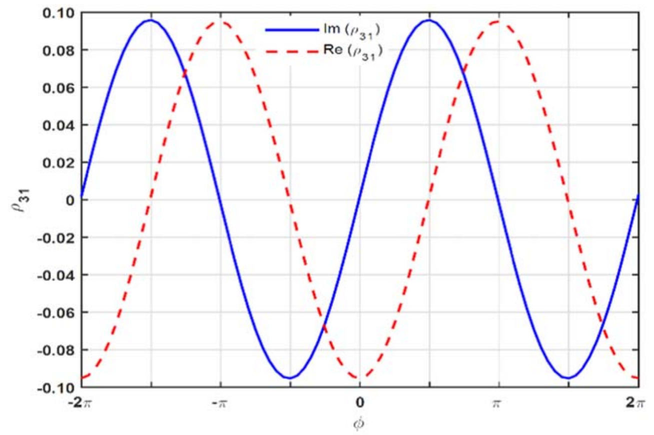

Figure 2. Plots of absorption (solid line) and dispersion (dashed line) versus the relative phase ϕ. The parameters were chosen as $\Omega_p = 0.5\gamma_{31}$, $\Omega_c = 10\gamma_{31}$, $\Omega_m = 1\gamma_{31}$, $\Delta_p = 0$, $\Delta_c = 0$, $\gamma_{32} = \gamma_{31}$, and $\gamma_{21} = 0$.

relative phase for a given set of values of the parameters Ω_{p}, Ω_{m}, and Ω_{c}.

In the following, we solved the coupled Bloch–Maxwell equations (2*a*)–(2*g*) on a space–time grid by a combination of the four-order Runge–Kutta and finite difference methods for the initial condition at which all atoms are in the ground state $|1\rangle$, and for the boundary condition at which the initial probe field is a continuous wave (*cw*) at the entrance of the medium. We used the relative phase $\phi(\tau)$ to inform a nearly square wave with smooth rising and falling edges in four ranges: 0 to $\pi/2$, $\pi/2$ to π, π to $3\pi/2$, and $3\pi/2$ to 2π [42]:

$$\begin{aligned}\phi(\tau) = \pi/2\{&a_n - 0.5[\tanh 0.4(\tau - 10)\\ &- \tanh 0.4(\tau - 35) + \tanh 0.4(\tau - 60)\\ &- \tanh 0.4(\tau - 85)]\}.\end{aligned} \quad (3)$$

Here, $a_n = 1, 2, 3$, and 4, corresponding to the ranges 0-$\pi/2$, $\pi/2$-π, π-$3\pi/2$, and $3\pi/2$-2π, respectively. Figure 3 shows a switching process of the probe field at $\xi = 50/\alpha$ inside the medium, where the probe transmission is switched to a nearly square pulse train depending on the switching range of the relative phase. Indeed, in the ranges 0-$\pi/2$ and $3\pi/2$-2π, the probe intensity is switched anti-synchronously with the modulation mode of the relative phase (figures 3(a), (d)). However, in the ranges $\pi/2$-π and $3\pi/2$-2π of the relative phase, the probe is switched synchronously with the relative phase (figures 3(b), (c)). By comparing these ranges of switching modes with the absorption curve in figure 2, one can see that the probe field is switched synchronously or anti-synchronously (with the switching of the relative phase) in the region of decreasing or increasing absorption, respectively.

It should be emphasized from figure 3 that the switched probe pulses oscillate at the beginning before reaching a steady square shape. In order to explain this dynamical trend, we plotted the absorption coefficient, Im(ρ_{31}), versus time as shown in figure 4. It shows temporal changes at the beginning, where the absorption curve oscillates before reaching a steady regime. This means that the switching process is governed by atomic dynamics with a time order of $1/\gamma_{31}$.

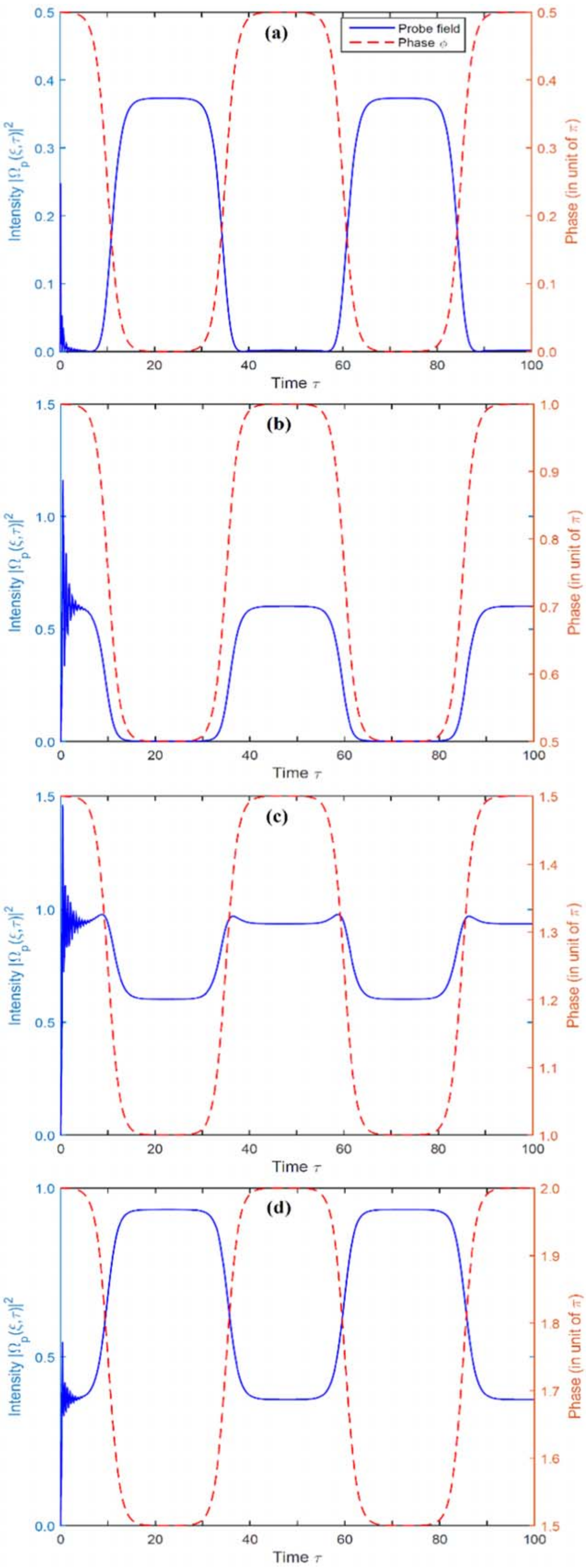

Figure 3. Time evolution of a *cw* probe field (solid line) at $\xi = 50/\alpha$ versus time τ under modulation of the relative phase $\phi(\tau)$ (dashed lines) given by equation (3) in the ranges 0-$\pi/2$ (a), $\pi/2$-π (b), π-$3\pi/2$ (c), and $3\pi/2$-2π (d). Other parameters are given by $\Omega_p = 0.5\gamma_{31}$, $\Omega_c = 10\gamma_{31}$, $\Omega_m = \gamma_{31}$, $\Delta_p = \Delta_c = 0$, $\gamma_{32} = \gamma_{31}$, *and* $\gamma_{21} = 0$.

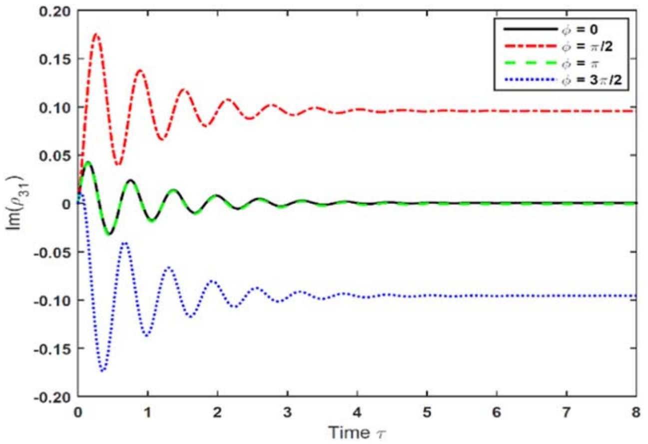

Figure 4. Temporal evolution of absorption versus time when $\phi = 0$ (solid line), $\phi = \pi/2$ (dot-dashed line), $\phi = \pi$ (dashed line), and $\phi = 3\pi/2$ (dotted line). Other parameters are the same as in figure 2.

Next, we considered how the transmitted probe field at $\xi = 50/\alpha$ changed with variation of the switching period of the microwave field, as shown in figure 5. Here, the switching period is determined via modulation of the Rabi frequency of the microwave field.

$$\Omega_m^{(i)}(\tau) = \Omega_{m0}\{1 - 0.5[\tanh(a_i\tau - 4) - \tanh(a_i\tau - 14) + \tanh(a_i\tau - 24) - \tanh(a_i\tau - 34)]\}, \quad (4)$$

where $a_1 = 0.4$, $a_2 = 1.0$, $a_3 = 2.0$, and $a_4 = 4.0$, corresponding to the switching periods $50/\gamma_{31}$, $20/\gamma_{31}$, $10/\gamma_{31}$, and $5/\gamma_{31}$, respectively. As shown in figure 5, the probe transmission is switched anti-synchronously with the switching microwave field. Furthermore, as the switching period decreases from $50/\gamma_{31}$ to $5/\gamma_{31}$ the first few transmitted probe pulses are disturbed out of the nearly square shape. However, when the steady regime is established, the switching shape can remain (figure 5(c)). Such distortion of the probe pulses is consistent with the evolution of absorption in the case of $\phi = \pi/2$ (figure 4), which is governed by the lifetime of the atomic state (inversely proportional to decay rates).

It should be noted from figure 5 that the medium becomes strongly absorptive when the microwave is present (the microwave pulses are opened), thus corresponding to the case of electromagnetically induced absorption (EIA). However, when the microwave is absent (the microwave pulses are closed), the medium become transparent (EIT), which is consistent with EIT theory presented in [2]. Therefore, when $\phi = \pi/2$, by switching the microwave to ON or OFF mode the probe is switched respectively to OFF or ON, due to the medium being switched to EIA or EIT regime.

The influence of the intensity of the coupling light on the probe field is considered by plotting the temporal evolution of the transmitted probe field for different intensities of the coupling field, as shown in figure 6. By comparing the cases $\Omega_c = 5\gamma_{31}$ (figure 6(a)), $\Omega_c = 10\gamma_{31}$ (figure 5(a)), and $\Omega_c = 15\gamma_{31}$ (figure 6(b)), one can see that the highest switching efficiency is attained at $\Omega_c = 10\gamma_{31}$, whereas

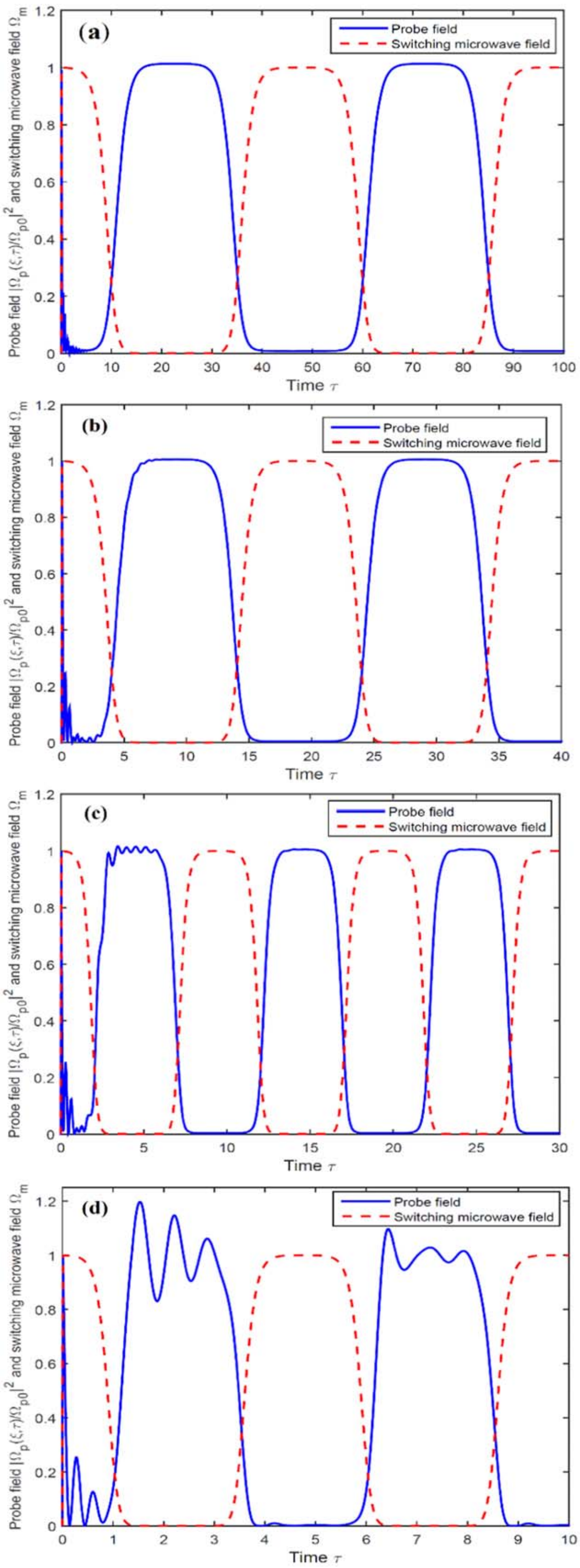

Figure 5. Temporal evolution of the transmitted probe field (solid line) and the switching microwave field (dashed line) at $\xi = 50/\alpha$ for different switching periods: (a) $50/\gamma_{31}$; (b) $20/\gamma_{31}$; (c) $10/\gamma_{31}$; and (d) $5/\gamma_{31}$. The other parameters are $\phi = \pi/2$, $\Omega_p = 0.5\gamma_{31}$, $\Omega_c = 10\gamma_{31}$, $\Omega_{m0} = \gamma_{31}$, $\Delta_p = 0$, $\Delta_c = 0$, $\gamma_{32} = \gamma_{31}$, and $\gamma_{21} = 0$.

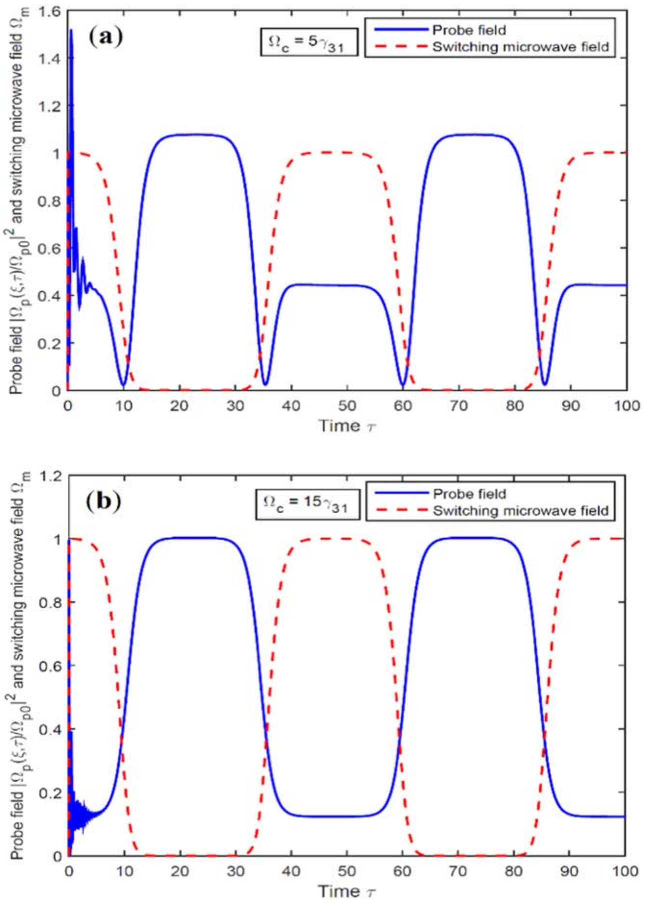

Figure 6. Temporal evolution of the probe field (solid line) at $\xi = 50/\alpha$ for $\Omega_c = 5\gamma_{31}$ (a) and $\Omega_c = 15\gamma_{31}$ (b). Other parameters are $\phi = \pi/2$, $\Omega_p = 0.5\gamma_{31}$, $\Omega_{m0} = \gamma_{31}$, $\Delta_p = 0$, $\Delta_c = 0$, $\gamma_{32} = \gamma_{31}$, and $\gamma_{21} = 0$.

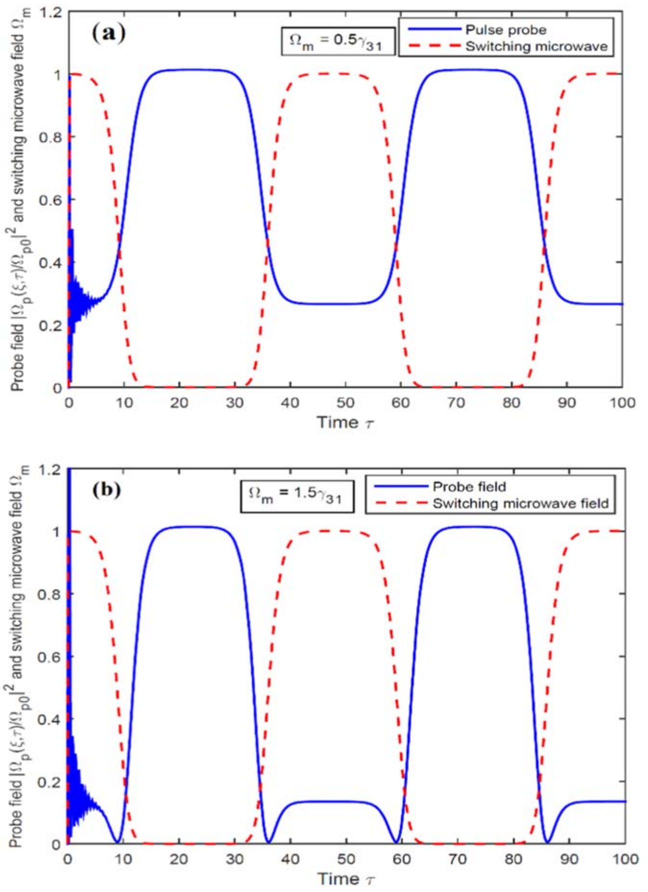

Figure 7. Time evolution of the probe field (solid line) at $\xi = 50/\alpha$ for different intensities of the microwave field: $\Omega_{m0} = 0.5\gamma_{31}$; (b) $\Omega_{m0} = 1.5\gamma_{31}$. The other parameters are $\phi = \pi/2$, $\Omega_c = 10\gamma_{31}$, $\Omega_p = 0.5\gamma_{31}$, $\Delta_p = 0$, $\Delta_c = 0$, $\gamma_{32} = \gamma_{31}$, and $\gamma_{21} = 0$.

smaller or larger coupling intensity may lead to lower switching efficiency.

We then consider the influence of the microwave field intensity on the switching by plotting the temporal evolution of the probe field for two cases, $\Omega_{m0} = 0.5\gamma_{31}$ and $\Omega_{m0} = 1.5\gamma_{31}$, as shown in figure 7. By comparing figure 5(a) with figure 7 one can see the sensitive influence of the microwave intensity on the transmitted probe field. This is due to the microwave field changing significantly the coherence between states $|1\rangle$ and $|2\rangle$.

The above results were obtained with an assumption that the decay between the two lower states vanished (i.e. $\gamma_{21} = 0$). Although the amplitude of γ_{21} for the case of the lambda configuration is often much smaller than the cases of V-shaped and ladder types, it should be taken into account for the case of low intensity of the probe light. In figure 8 we plot the probe field at different values of γ_{21}, namely, $\gamma_{21} = 0.1\gamma_{31}$, $10\gamma_{31}$, and $50\gamma_{31}$. It shows that a larger value of γ_{21} leads to a lower intensity of the switched probe pulse, thus reducing switching efficiency. Therefore, the three-level lambda atomic medium with a small decay rate is favorable for applications of switching at a low level of light intensity.

Finally, by looking the overall results in figures 2–8 one can see only particular value regions of the parameters which

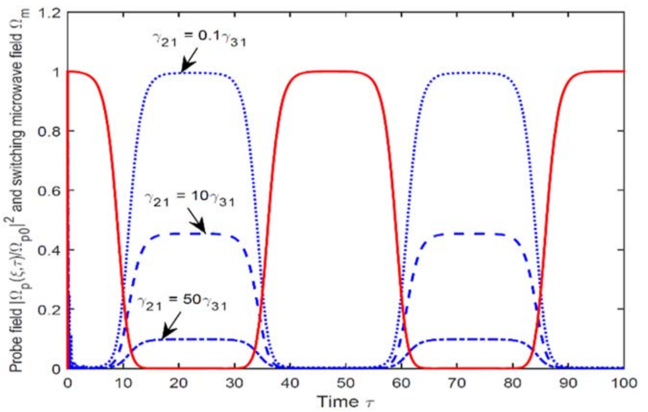

Figure 8. Variation of the transmitted probe field at $\xi = 50/\alpha$ for different decay rates: $\gamma_{21} = 0.1\gamma_{31}$ (dotted line), $\gamma_{21} = 10\gamma_{31}$ (dashed line), and $\gamma_{21} = 50\gamma_{31}$ (dot-dashed line), when the microwave field (solid line) is switched at the period $50/\gamma_{31}$. The remaining parameters are the same as in figure 5.

can switch the *cw* probe field into the pulse train, either synchronously or asynchronously with the switched phase. As indicated in [45], the relative intensities of the applying fields to obtain high-contrast optical switching (or high switching efficiency) are $\Omega_p \ll \Omega_m \ll \Omega_c$. This inequality comes from conditions for EIT establishment [2, 3], which is consistent with the case of having high-contrast switching in this work (figure 5(a)), namely, $\Omega_p = 0.5\gamma_{31}$, $\Omega_m = \gamma_{31}$, $\Omega_c = 10\gamma_{31}$. However, the conditions given in [45] should be further restricted and accompanied with others. Indeed, when increasing $\Omega_c = 15\gamma_{31}$ (figure 6(b)) or when increasing $\Omega_m = 1.5\gamma_{31}$ (figure 7(b)), the switching efficiency is lower; when reducing the switching cycle (figure 5), the first few switched probe pulses are disturbed.

4. Possible experimental realization

In this section, we provide a possible realization of optical switching in the closed-loop three-level lambda system. In principle, the closed-loop three-level lambda scheme can be applied to any atomic or molecular system having a similar level structure to that in figure 1. Here, we propose the case of ^{87}Rb atomic gas contained in a pyrex cell, which is convenient for low-cost single-mode external cavity diode lasers. The experimental arrangement can be similar to that described in [44, 45] for the cases of switching based on the relative phase. Here, the states $|1\rangle$, $|2\rangle$, and $|3\rangle$ can be chosen by the hyperfine states $5S_{1/2}$ ($F = 1$), $5P_{1/2}$ ($F = 1$), and $5S_{1/2}$ ($F = 2$), respectively [47]. However, for consideration of the influence of intensity of the coupling light, switching rate of the microwave, and coupling intensity, one should use additional elements. Indeed, a combination of waveplate and polarizer may be employed to vary the intensity of the coupling field, whereas two variable choppers can be used to switch the coupling and microwave intensity into pulses.

5. Conclusions

We have proposed a model of optical switching in a closed-loop three-level lambda system excited by a microwave and two pump and probe optical fields. The behavior of the switching is studied under modulation of the relative phase range, microwave, and coupling fields. It is shown that transmission of the continuous probe field can be switched to a nearly square pulse train with the same modulation period of the relative phase. In addition to the phase control, the probe field can also be switched to pulse trains by modulating the microwave field in which its switching efficiency is sensitive with the microwave intensity and decay rate of the atomic state. Such controllable optical switching in a closed-loop three-level system provides the possibility of phase-controlled and intensity switching operations which are suitable for realizing optical switching and amplification devices working at low light levels.

Acknowledgments

The financial support from the Ministry of Science and Technology through the grant code ĐTĐLCN.17/17 is acknowledged.

ORCID iDs

Huy Bang Nguyen https://orcid.org/0000-0003-4702-3157

References

[1] Ishikawa H 2008 *Ultrafast All-Optical Signal Processing Devices* (Singapore: John Wiley & Sons)
[2] Imamoğlu A and Harris S E 1989 Lasers without inversion: interference of dressed lifetime broadened states *Opt. Lett.* **14** 1344–6
[3] Boller K J, Imamoglu A and Harris S E 1991 Observation of electromagnetically induced transparency *Phys. Rev. Lett.* **66** 2593
[4] Harris S E and Yamamoto Y 1998 Photon Switching by Quantum Interference *Phys. Rev. Lett.* **81** 3611
[5] Schmidt H and Ram R J 2000 All-optical wavelength converter and switch based on electromagnetically induced transparency *Appl. Phys. Lett.* **76** 3173
[6] Fountoulakis A, Terzis A F and Paspalakis E 2010 All-optical modulation based on electromagnetically induced transparency *Phys. Lett.* A **374** 3354
[7] Yan M, Rickey E G and Zhu Y 2001 Observation of absorptive photon switching by quantum interference *Phys. Rev.* A **64** 041801 (R)
[8] Antón M A, Calderón O G, Melle S, Gonzalo I and Carreño F 2006 All-optical switching and storage in a four-level tripod-type atomic system *Opt. Commun.* **268** 146
[9] Khoa D X, Doai L V, Anh L N M, Trung L C, Thuan P V, Dung N T and Bang N H 2016 Optical bistability in a five-level cascade EIT medium: an analytical approach *J. Opt. Soc. Am.* B **33** 735
[10] Sheng J, Yang X, Khadka U and Xiao M 2011 All-optical switching in an N-type foul-level atom-cavity system *Opt. Express* **19** 17059–64
[11] Jafarzadeh H 2017 All-optical switching in an open V-type atomic system *Laser Phys.* **27** 025204
[12] Fleischhauer M, Imamoglu A and Marangos J P 2005 Electromagnetically induced transparency: optics in coherent media *Rev. Mod. Phys.* **77** 633
[13] Doai L V, Trong P V, Khoa D X and Bang N H 2014 Electromagnetically induced transparency in five-level cascade scheme of 85Rb atoms: an analytical approach *Optik* **125** 3666
[14] Khoa D X, Trung L C, Thuan P V, Doai L V and Bang N H 2017 Measurement of dispersive profile of a multi-window EIT spectrum in a Doppler-broadened atomic medium *J. Opt. Soc. Am.* B **34** 1255
[15] Khoa D X, Doai L V, Son D H and Bang N H 2014 Enhancement of self-Kerr nonlinearity via electromagnetically induced transparency in a five-level cascade system: an analytical approach *J. Opt. Soc. Am.* B **31** 1330
[16] Doai L V, Khoa D X and Bang N H 2015 EIT enhanced self-Kerr nonlinearity in the three-level lambda system under Doppler broadening *Phys. Scr.* **90** 045502
[17] Hamedi H R, Gharamaleki A H and Sahrai M 2016 Colossal Kerr nonlinearity based on electromagnetically induced transparency in a five-level double-ladder atomic system *Appl. Opt.* **22** 5892
[18] Shiau B-W, Wu M-C, Lin C-C and Chen Y-C 2011 Low-light-level cross-phase modulation with double slow light pulses *Phys. Rev. Lett.* **106** 193006

[19] Venkataraman V, Saha K and Gaeta A L 2013 Phase modulation at the few-photon level for weak-nonlinearity-based quantum computing *Nat. Photon.* **7** 138–41
[20] Huang G, Jiang K, Payne M G and Deng L 2006 Formation and propagation of coupled ultraslow optical soliton pairs in a cold three-state double-Λ-system *Phys. Rev.* E **73** 056606
[21] Yu R, Li J, Huang P, Zheng A and Yang X 2009 Dynamic control of light propagation and optical switching through an RF-driven cascade-type atomic medium *Phys. Lett.* A **373** 2992
[22] Si L-G, Lu X-Y, Hao X and Li J-H 2010 Dynamical control of soliton formation and propagation in a Y-type atomic system with dual ladder-type electromagnetically induced transparency *J. Phys. B: At. Mol. Opt. Phys.* **43** 065403
[23] Yu R, Li J, Ding C and Yang X 2011 Dual-channel all-optical switching with tunable frequency in a five-level double-ladder atomic system *Opt. Commun.* **284** 2930
[24] Chen Y, Bai Z and Huang G 2014 Ultraslow optical solitons and their storage and retrieval in an ultracold ladder-type atomic system *Phys. Rev.* A **89** 023835
[25] Dong H M, Doai L V, Sau V N, Khoa D X and Bang N H 2016 Propagation of laser pulse in a three-level cascade atomic medium under conditions of electromagnetically induced transparency *Photonics Letters of Poland* **3** 73
[26] Khoa D X, Dong H M, Doai L V and Bang N H 2017 Propagation of laser pulse in a three-level cascade inhomogeneously broadened medium under electromagnetically induced transparency conditions *Optik* **131** 497
[27] Hamedi H R 2017 Optical switching, bistability and pulse propagation in five-level quantum schemes *Laser Phys.* **27** 066002
[28] Dong H M, Doai L V and Bang N H 2018 Pulse propagation in an atomic medium under spontaneously generated coherence, incoherent pumping, and relative laser phase *Opt. Commun.* **426** 553–7
[29] Korsunsky E A, Leinfellner N, Huss A, Baluschev S and Windholz L 1999 Phase-dependent electromagnetically induced transparency *Phys. Rev.* A **59** 2302
[30] Bortman-Arbiv D, Wilson-Gordon A D and Friedmann H 2001 Phase control of group velocity: from subluminal to superluminal light propagation *Phys. Rev.* A **63** 043818
[31] Xu W H, Wu J H and Gao J Y 2003 Phase-dependent properties in a microwave-driven V system: gain without population inversion and narrow resonances *Opt. Commun.* **223** 367–73
[32] Liu C, Gong S, Nakajima T and Xu Z 2006 Phase-sensitive atom localization in a loop Λ-system *J. Mod. Opt.* **12** 1791–802
[33] Sun H, Niu Y P, Jin S Q and Gong S Q 2007 Phase control of cross-phase modulation with electromagnetically induced transparency *J. Phys. B: At. Mol. Opt. Phys.* **40** 3037
[34] Sun H, Niu Y P, Jin S Q and Gong S Q 2008 Phase control of the Kerr nonlinearity in electromagnetically induced transparency media *J. Phys. B: At. Mol. Opt. Phys.* **41** 065504
[35] Qi Y, Niu Y, Zhou F, Peng Y and Gong S 2011 Phase control of coherent pulse propagation and switching based on electromagnetically induced transparency in a four-level atomic system *J. Phys. B: At. Mol. Opt. Phys.* **44** 085502
[36] Xu W H, Wu J H, Gao J Y and Zhang B 2003 Elimination of the transient absorption in a microwave-driven Λ-type atomic system *Phys. Lett.* A **314** 23–8
[37] Zeng Z Q, Wang Y-P and Hou B P 2013 Amplitude and phase control of transient absorption and dispersion in a microwave-driven atomic system *Eur. Phys. J.* D **67** 76
[38] Cheng D-C, Liu C-P and Gong S-Q 2006 Optical bistability via amplitude and phase control of a microwave field *Opt. Commun.* **263** 111–5
[39] Agarwal G S, Dey T N and Menon S 2001 Knob for changing light propagation from subluminal to superluminal *Phys. Rev.* A **64** 053809
[40] Jiahua Li 2007 Coherent control of optical bistability in a microwave-driven V-type atomic system *Physica* D **228** 148–52
[41] Kou J, Wan R G, Kang Z H, Jiang L, Wang L, Jiang Y and Gao J Y 2011 Phase-dependent coherent population trapping and optical switching *Phys. Rev.* A **84** 063807
[42] Li J H, Yu R and Yang X 2013 Phase-controlled absorption-gain properties and optical switching in nanodiamond nitrogen-vacancy center *Appl. Phys.* B **111** 65–73
[43] Morigi G, Franke-Arnold S and Oppo G-L 2002 Phase-dependent interaction in a four-level atomic configuration *Phys. Rev.* A **66** 053409
[44] Kang H, Hernandez G, Zhang J and Zhu Y 2006 Phase-controlled light switching at low light levels *Phys. Rev.* A **73** 011802 (R)
[45] Ghosh M, Karigowda A, Jayaraman A, Bretenaker F, Sanders B C and Narayanan A 2017 Demonstration of a high-contrast optical switching in an atomic Delta system *J. Phys. B: At. Mol. Opt. Phys.* **50** 165502
[46] Suter D 1997 *The Physics of Laser-Atom Interactions* (Cambridge: Cambridge University Press)
[47] Steck D A 'Rubidium ^{87}D Line Data,' available online at http://steck.us/alkalidata